Acoustic Analysis of a High-Frequency Ultrasonic Cleaner

*Sunghoon Choi, *Jin Oh Kim, and **Yong-Hoon Kim

Abstract

Ultrasonic cleaning at high frequency around 1 MHz, called megasonic cleaning, is commonly used to remove particles less than 1 μm by generating high frequency accelerations on the cleaning objects. Cleaning is performed in an ultrasonically-excited liquid contained in a double-structured container. Ultrasonic waves generated by piezoelectric transducers propagate in the outer container and are transmitted through the inner container. The bottom of the inner container is inclined to make oblique incidence of the ultrasonic wave in order to raise the efficiency of the wave transmission through the bottom plate. This work deals with the efficiency of the wave transmission, which directly affects the cleaning performance. The transmission characteristics of the ultrasonic wave in the megasonic cleaner have been obtained analytically and numerically for the variations of some parameters, such as the thickness and inclined angle of the bottom plate of the inner container and the chemical ratio and temperature of the cleaning liquid. The calculated results have yielded the optimum cleaning condition in terms of the sound power transmitted into the cleaning liquid.

I. Introduction

Ultrasonic cleaning is an efficient method removing unwanted particles from an object by exerting mechanical oscillations of high frequency. Ultrasonic cleaners used in manufacturing lines are mostly composed of an electrical oscillator and a mechanical vibrator. The mechanical vibrator, whose transducers transform an electrical oscillation signal into a mechanical vibration, is submerged in or attached to a cleaning tank which contains a cleaning liquid. The object to be cleaned is immersed in the cleaning liquid.

The cleaning mechanisms are based on the high-frequency acceleration and the cavitation in a cleaning liquid [1]. The ultrasonic cleaner operated at the frequency range of several decade kHz relies mostly on the cavitation mechanism. This kind of ultrasonic cleaner is suitable to remove dirty particles of several μm order, and is used for example for the cleaning of shadow masks, which are parts of the Brown tubes. A study to reduce the erosion damage on the vibrator caused by the cavitation and to improve the cleaning performance of this type was reported earlier [2]. Meanwhile, the cleaner removing much smaller particles, such as 1 μm or less, and preventing cavitation damage is operated at much higher frequency, say around 1 MHz. This kind of cleaner relies mostly on the high-frequency acceleration force [3] and is used for example in the semiconductor production for the cleaning of photo masks or silicon wafers.

The ultrasonic cleaner considered in this paper is operated at 1 MHz, and is called a megasonic cleaner [4]. Cleaning is performed in an ultrasonically-excited liquid contained in a double-structured container, whose inner container is made of a non-metallic material such as fused quartz or pyrex glass so as to isolate the cleaning object from metallic ions. Ultrasonic waves generated by piezoelectric transducers propagate in the outer container and are transmitted through the inner container. The cleaning performance is directly affected by the sound power in the inner container. As shown in Fig. 1, the bottom of the inner container is inclined to make oblique incidence of the ultrasonic wave in order to raise the efficiency of the wave transmission through the bottom plate [5].

This paper deals with the efficiency of the wave transmission by analytical and numerical approaches. The transmission efficiency is calculated analytically by considering the interactions of waves in an elastic plate of infinite length and liquids in contacts with the plate. The transmission characteristics of the ultrasonic wave is obtained for the variations of some parameters, such as the thickness and inclined angle of the bottom plate of the inner container and the chemical ratio and temperature of the cleaning liquid. Numerical calculations are performed by combining the finite element analysis of the vibration of the inner container and the boundary element analysis of the pressure field in the cleaning liquid.

*Supercomputing Applications Lab., Samsung Advanced Institute of Technology
**Semiconductor R&D Center, Samsung Electronics

Manuscript Received: April 21, 1997.

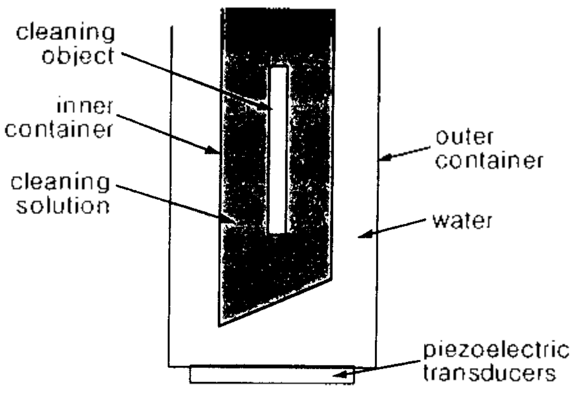

Figure 1. Cross-sectional diagram of a high-frequency ultrasonic cleaner with inner container.

Ⅱ. Wave Transmission through an Inclined Plate

2.1 Wave Theory

The transmission and reflection of the plane waves incident obliquely on the infinite plate immersed in liquids as shown in Fig. 2 can be described in terms of the scalar potential ϕ and one component of the vector potential ψ of the displacements [6, 7]. The components u and w of the particle displacements in the x-and z-axis directions respectively are expressed as

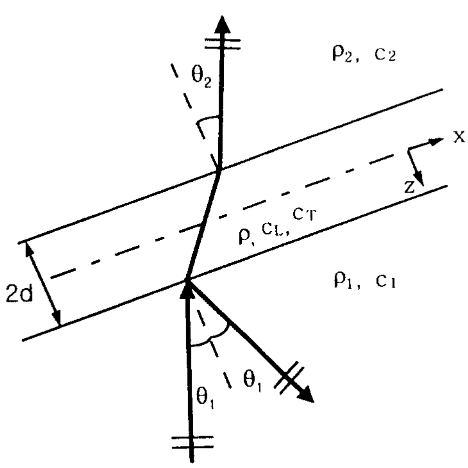

Figure 2. Schematic diagram of the transmission and reflection of obliquely-incident plane waves on a plate.

$$u=\frac{\partial\phi}{\partial x}-\frac{\partial\psi}{\partial z} \tag{1}$$

$$w=\frac{\partial\phi}{\partial z}+\frac{\partial\psi}{\partial x} \tag{2}$$

in the elastic plate. The normal stress σ_z and shear stress τ_{xz} are expressed as

$$\sigma_z=\lambda\left(\frac{\partial^2\phi}{\partial x^2}+\frac{\partial^2\phi}{\partial z^2}\right)+2\mu\left(\frac{\partial^2\phi}{\partial z^2}+\frac{\partial^2\psi}{\partial x\partial z}\right) \tag{3}$$

$$\tau_{xz}=\mu\left(2\frac{\partial^2\phi}{\partial x\partial z}+\frac{\partial^2\psi}{\partial x^2}-\frac{\partial^2\psi}{\partial z^2}\right) \tag{4}$$

where λ and μ are Lame constants.

The potentials ϕ and ψ satisfy the following two-dimensional wave equations.

$$\frac{\partial^2\phi}{\partial x^2}+\frac{\partial^2\phi}{\partial z^2}=\frac{1}{c_L^2}\frac{\partial^2\phi}{\partial t^2} \tag{5}$$

$$\frac{\partial^2\psi}{\partial x^2}+\frac{\partial^2\psi}{\partial z^2}=\frac{1}{c_T^2}\frac{\partial^2\psi}{\partial t^2} \tag{6}$$

where c_L $(=[(\lambda+2\mu)/\rho]^{1/2})$ and c_T $(=[\mu/\rho]^{1/2})$ are the velocities of longitudinal and transverse waves, respectively, and ρ is the mass density of the plate. For the angular frequency ω and wave velocities c_L and c_T, the wavenumbers k_L $(=\omega/c_L)$ and k_T $(=\omega/c_T)$ are used for later derivation. The wave in the elastic plate, which is called Lamb wave, has the solution of the following form.

$$\phi=[A_s\cosh(qz)+B_a\sinh(qz)]\exp[i(kx-\omega t)] \tag{7}$$

$$\psi=[C_a\cosh(sz)+D_s\sinh(sz)]\exp[i(kx-\omega t)] \tag{8}$$

where A_s, B_a, C_a, D_s are arbitrary constants and $q^2=(k^2-k_L^2)^{1/2}$, $s^2=(k^2-k_T^2)^{1/2}$. The plane wave in a liquid can be expressed in terms of the scalar potential only.

The incident wave potential ϕ_I, reflected wave potential ϕ_R, and transmitted wave potential ϕ_T, which satisfy the wave equation (Eq. (5)), have the solutions of the following forms.

$$\phi_I=\Phi_I\exp[i\,k_1(\sin\theta_1 x-\cos\theta_1 z)-i\omega t] \tag{9}$$

$$\phi_R=\Phi_R\exp[i\,k_1(\sin\theta_1 x+\cos\theta_1 z)-i\omega t] \tag{10}$$

$$\phi_T=\Phi_T\exp[i\,k_2(\sin\theta_2 x-\cos\theta_2 z)-i\omega t] \tag{11}$$

where $k_1=\omega/c_1$, $k_2=\omega/c_2$, and c_1 and c_2 are respectively the velocities of the acoustic waves in liquid 1 and liquid 2 of Fig. 2. In a liquid i $(i=1, 2)$ the acoustic pressure is $p=-\rho_i\omega^2\phi$, where ρ_i is the mass density of fluid i, and the displacements are $u=\partial\phi/\partial x$ and $w=\partial\phi/\partial z$.

At the interfaces (z = ±d) between the elastic plate and the non-viscous liquids, the normal component of the displacement is continuous. At the interfaces the normal component of the stress σ_z is equivalent to the acoustic pressure and the shear stress τ_{xz} is zero. Introducing Eqs. (7)-(11) into six boundary conditions, three at z = −d and three at z = d, yields the following matrix equation.

$$\begin{bmatrix} H_{11} & H_{12} & H_{13} & H_{14} & H_{15} & H_{16} \\ H_{21} & H_{22} & H_{23} & H_{24} & H_{25} & H_{26} \\ H_{31} & H_{32} & H_{33} & H_{34} & H_{35} & H_{36} \\ H_{41} & H_{42} & H_{43} & H_{44} & H_{45} & H_{46} \\ H_{51} & H_{52} & H_{53} & H_{54} & H_{55} & H_{56} \\ H_{61} & H_{62} & H_{63} & H_{64} & H_{65} & H_{66} \end{bmatrix} \begin{Bmatrix} A_s \\ B_a \\ C_a \\ D_s \\ \Phi_R \\ \Phi_T \end{Bmatrix} = \begin{Bmatrix} ik_1\cos\theta_1 \exp(-ik_1\cos\theta_1)\Phi_I \\ 0 \\ 0 \\ 0 \\ -(\rho_1/\rho)k_T^2 \exp(-ik_1\cos\theta_1)\Phi_I \\ 0 \end{Bmatrix} \tag{12}$$

where the elements H_{ij} of the 6×6 matrix $[H]$ are written in Appendix. The amplitude of the transmitted wave ϕ_T can be calculated relative to the amplitude of the incident wave ϕ_I from Eq. (12).

2.2 Dependence on the Plate Thickness and Inclination

The transmission ratio of the elastic waves propagating from a liquid through a plate into another liquid is defined as $|\Phi_T/\Phi_I|$. As shown in Eq. (12), the transmission ratio depends on the plate thickness and the oblique angle of the incident wave as well as on the material properties of the media and the wave frequency. In this research the frequency of the elastic wave generated in the cleaner is 1 MHz. The material of the inner container was fused quartz, and the material properties of the plate are mass density $\rho = 2{,}200$ kg/m^3, longitudinal wave speed $c_L = 5{,}900$ m/s, and transverse wave speed $c_T = 3{,}750$ m/s [8]. The liquid in the region of the incident wave, i.e. in the outer container, is pure water and the liquid in the region of the transmitted wave, i.e. in the inner container, is a solution of pure water including small amount of chemicals. The mass density and wave speed measured at 40℃ as described in the next section are $\rho_1 = 983$ kg/m^3 and $c_1 = 1{,}530$ m/s in the pure water and $\rho_2 = 985$ kg/m^3 and $c_2 = 1{,}530$ m/s, respectively.

Transmission ratio has been calculated with Eq. (12) for various plate thickness and wave incidence angle and the results are shown in Fig. 3. Figure 3(a) displays the transmission ratio of an incident wave through an inclined plate an a function of the incident angle for several plate thickness, while Fig. 3(b) displays the contour plot of the transmission ratio as a function of the incident angle and the plate thickness. Each curve in Fig. 3(a) shows peaks at several values of the incident angle. This result is consistent with the experimental observation [9]. This phenomenon, the transmission characteristics of the wave through a plate of finite thickness, can be explained in terms of the dispersion of Lamb wave speed, which depends on the plate thickness and the frequency [7]. Since the wave frequency of 1 MHz is fixed, only the effect of the various thickness is considered below.

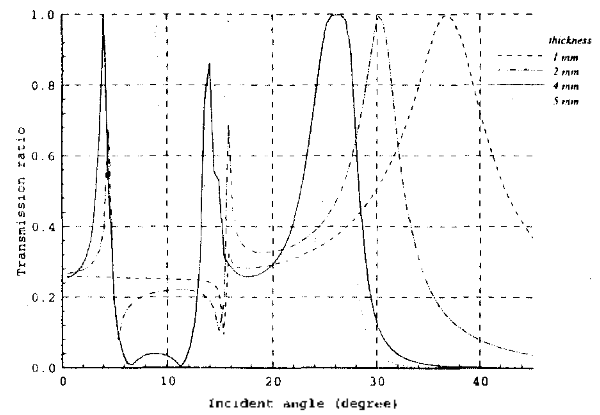

(a)

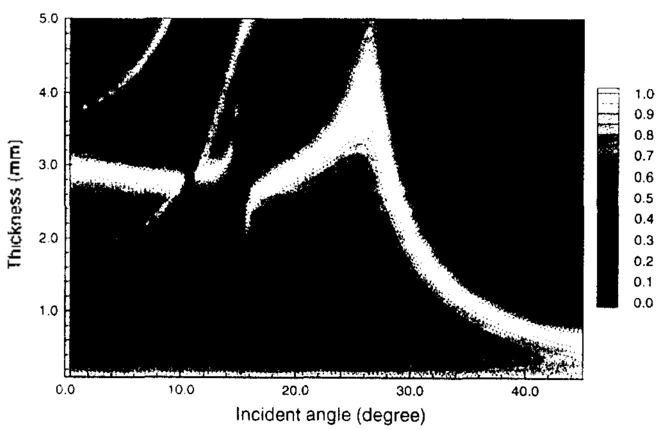

(b)

Figure 3. Transmission ratio of an incident wave through an inclined plate. (a) Variation of the transmission ratio as a function of the incident angle for several plate thickness. (b) Contour plot of the transmission ratio as a function of the incident angle and the thickness of the plate.

Lamb waves, which propagate along a plate and have motion components in the directions of surface normal and wave propagation, are affected by the adjacent liquids in case the plate is immersed in liquid media as shown in Fig. 2. Such waves are called leaky Lamb waves because of the leakage of wave energy into the liquid. Leaky Lamb waves are described by Eq. (12) with $\Phi_I = 0$ and the characteristic equation is obtained when the determinant of matrix $[H]$ is set equal to zero. The solutions of the characteristic equation represent symmetric modes s_0, s_1, s_2, ... and antisymmetric modes a_0, a_1, a_2, ..., and the wavelength of each mode can be found.

The continuity of the wave motion at the interface between the plate and the liquid implies that the displacement components of the plate and the liquid in the surface normal direction are equal to each other. Thus the wavelength λ_2 of the elastic wave excited by the incidence of the wave from the liquid is determined by the wavelength λ_1 in the liquid and the incident angle θ_1 as shown in Fig. 4 with the relation $\lambda_2 = \lambda_1/\sin\theta_1$. As the λ_2 value approaches the wavelength of a leaky Lamb wave mode, the incident wave excites the elastic wave in the plate efficiently. As the incident angle decreases, the higher mode of the larger wave speed is excited since the λ_2 value increases. The first peak from the right of each curve in Fig. 3(a) corresponds to the fundamental antisymmetric mode a_0 and the second and third peaks correspond to s_0 and a_1 modes, respectively. Each curve has different locations of the peaks because the dispersion characteristic of the Lamb waves is affected by the plate thickness also.

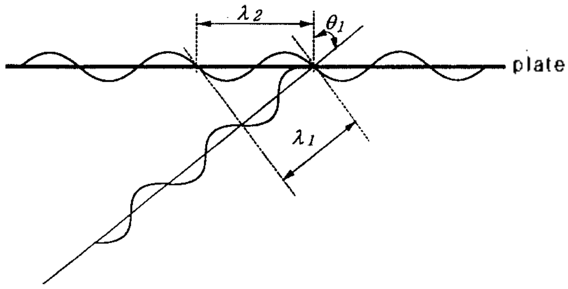

Figure 4. Relation between the incident waves in the liquid and the waves generated in the plate.

2.3 Effect of the Cleaning Liquid

The transmission of the ultrasonic wave is affected not only by the geometric and material parameters of the plate but also by the mass density and wave speed in the adjacent liquids of the incident wave region and the transmitted wave region. The mass density and wave speed in the liquid are dependent on the temperature and the chemical ratio of the solution. The liquid in the region of the incident wave region, i.e. in the outer container, is pure water and the liquid in the region of the transmitted wave region, i.e. in the inner container, is a chemical solution of water including small amount of ammonia and hydrogen peroxide to promote the cleaning process chemically.

The wave speed has been measured for four kinds of liquids, such as pure water, liquids A, B, and C, at various temperatures, ranging from 20 to 60℃, approximately 10℃ apart. The liquids A, B, and C are composed of water (more than 90 volume%), hydrogen peroxide (less than 10%), and small amount of ammonia. The ratio of ammonia content in the liquids A, B, and C are 1:2.5:5. The wave speed has been obtained by measuring the time-of-flight of a pulse echo in each liquid. The mass density has been measured by the conventional method of measuring the mass and volume.

The difference in the wave speed due to the temperature change of 40℃ is about 50 m/s. Meanwhile, the difference of the wave speed for the variation of the chemical composition in the cleaning liquid is within 5 m/s, and thus its effect on the transmission ratio is relatively negligible. The transmission of the wave incident from a pure water and propagating through the plate into the liquid B has been calculated for the temperatures 20, 40, 60℃ of the liquid B, and the results are displayed in Fig. 5 as a function of the incident angle. It appears from Fig. 5 that 50 m/s difference in the wave speed yields 2° difference in the incident angle yielding maximum transmission ratio.

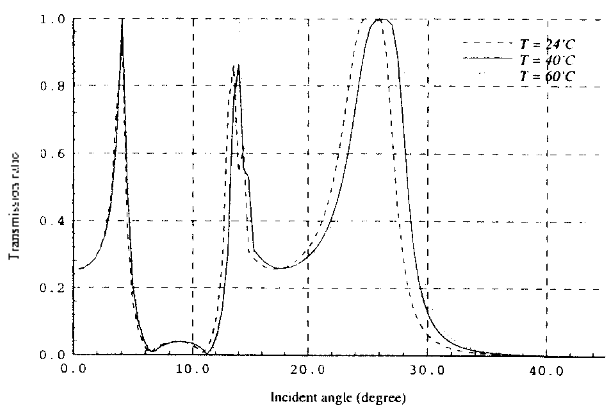

Figure 5. Transmission ratio of an incident wave through the plate of 4mm thickness at several liquid temperatures.

Ⅲ. Sound Pressure Distribution in the Cleaning Liquid

3.1 Numerical Analysis

The analysis carried out in the previous section is valid for an infinite plate. The geometry of the inner container of the ultrasonic cleaner is not simple enough to use a theoretical approach. As shown in Fig. 1 the bottom plate of the inner container is finite and the side walls may interact with the propagating waves. Therefore, the validity of the theoretical results in the previous section for the realistic shape of the ultrasonic cleaner shown in Fig. 1 must be verified numerically.

It is assumed that the ultrasonic waves generated at the bottom of the outer container by the transducers are plane waves and that there is no variation in the direction normal to the cross-section shown in Fig. 1. Thus two-dimensional analysis is good enough in this case. Since the motion of the plate is interacting with the motion of the adjacent liquids at both sides, a coupled analysis of the plate vibration and the liquid oscillation is necessary. Usually the finite element method (FEM) and the boundary element method (BEM) are used as convenient and powerful numerical schemes. A fully coupled analysis, which calculates the vibration of the container and the wave propagation in the liquid simultaneously, requires too many elements and too large computer capacity to be handled in the current hardware and software. Therefore, a one-way coupled analysis has been adopted for the numerical analysis as described below.

First of all, the vibration of the inner container excited by the incident plane waves has been calculated by using a commercial FEM software, ANSYS. The thickness of the bottom and walls of the inner container is 4 mm. The element size of the numerical model does not exceed 0.40 mm, which is less than 1/6 of the wavelength 3.75 mm of the transverse wave in fused quartz, the material of the inner container, in order to guarantee an accurate numerical analysis. The side walls of the inner container are almost not affected by the incident wave in the liquid of the outer container, and have been modeled as line elements with the boundary conditions of zero displacements. The excitation on the bottom plate of the inner container by the incident wave has been considered as external forces of a sinusoidal function. The magnitude and direction of the displacements at each nodal points of the bottom elements have been calculated by frequency-response analysis, and the example results are shown as a vector form in Fig. 6. This results is used in the acoustic analysis for the sound pressure distribution in the liquid in the inner container.

The acoustic field in the liquid of the inner container has been calculated by using a commercial BEM software, SYSNOISE. The element size of the boundary element model has been made not exceed 0.25 mm, which is about 1/6 of the wavelength of 1 MHz waves in water, in order to assure the accuracy of the numerical analysis. The conditions of the boundaries contacting with the inner container have been given from the calculated results of the container vibration. The free surface of the top face of the liquid, which requires zero acoustic pressure, has been conditioned by a sufficiently large value of admittance (10^5 $m^2/s/kg$) because the displacement boundary condition is not compatible with the pressure boundary condition in the direct BEM option of SYSNOISE. The bottom face has been conditioned by the vibration velocities converted from the displacements component normal to the bottom face. The material properties of the liquid are those of fluid B mentioned in Section 2.3.

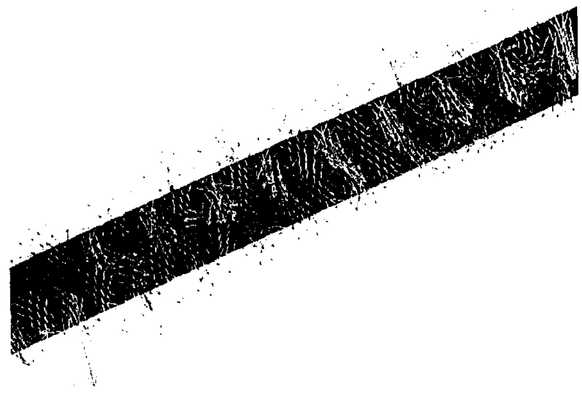

Figure 6. An example of the vibration analysis results showing the displacement in the bottom plate of the inner container.

3.2 Sound Pressure Distribution

The sound pressure distribution in the cleaning liquid of the inner container has been calculated by the procedure described in the previous section, and some of the results are shown in Fig. 7. Figure 7(a) is the result for the case of the inclined angle 28° and the temperature 40℃, while Fig. 7(b) is for the same geometry with a submerged object to be cleaned. The transmitted wave does not establish a standing wave field but a traveling wave field because of the inclination of the bottom plate of the inner container, and the sound pressure distribution shown in Fig. 7 is only an instantaneous snap shot of the waves in the cleaning liquid. The existence of the object in the cleaning liquid makes changes in the pattern of the sound pressure distribution but does not alter the overall level of the sound pressure. The meaning of the numerical analysis of the sound pressure distribution is explained below.

By calculating the sound pressure distribution in the cleaning liquid of the inner container, the transmission ratio of the wave through the bottom plate of the inner container has been obtained in terms of sound power transmission. The sound power transmitted through the bottom plate of the inner container has been calculated by integrating the sound intensity over the area of the inclined bottom face. This calculation has been carried out by using the 'contribution analysis' module of SYSNOISE, and the sound power $\bar{P}$ over the area S is given as follows.

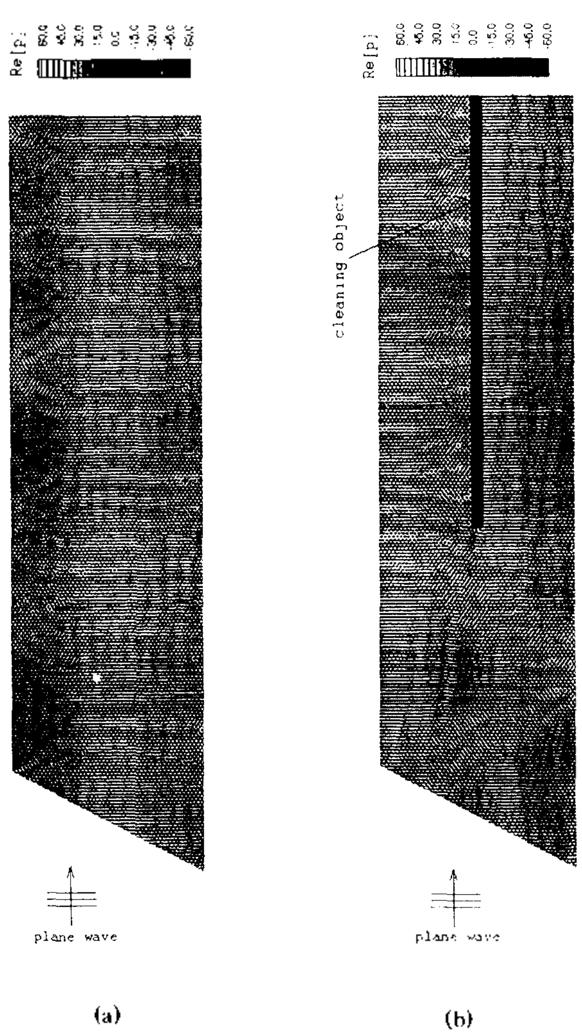

Figure 7. Sound pressure distributions in the liquid of the inner container: (a) without an object to be cleaned (b) with an object to be cleaned.

$$\bar{P}=\frac{1}{2}\int_{S}\mathrm{Re}[pv^{*}]\,dS \tag{13}$$

where p and v are the acoustic pressure and the particle velocity normal to the bottom face and (*) means complex conjugate.

By taking S to be the bottom plate of the boundary element model the sound power calculated by Eq. (13) represents the wave energy transmitted through the bottom plate into the cleaning liquid during a unit time. The calculated sound power in the liquid of 40℃ is displayed as a function of the inclined angle in Fig. 8(a). This result, obtained for the realistic finite region, is not identical to the theoretical curve in Fig. 3(a), which were obtained for the ideal infinite region. Both results, however, show a similar trend to each other. The best angle of the bottom inclination can be found from the result of Fig. 8(a).

If the inclined angle of the bottom plate is fixed and not easy to change, the second best way to raise up the wave transmission is the change of the liquid temperature. Another calculated result shown in Fig. 8(b) is the variation of the sound power as a function of the liquid temperature at a fixed inclination angle 24°. From this result it is possible to select the liquid temperature which allows the maximum transmission of the wave through the bottom plate of a fixed inclination angle.

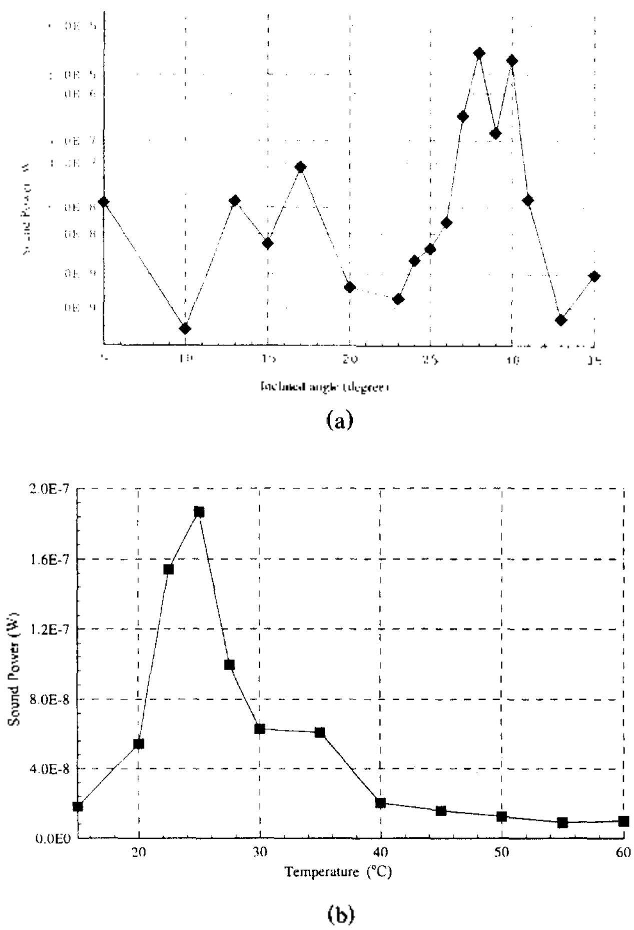

Figure 8. Radiated power of the wave transmitted through a 4-mm-thick bottom plate of the inner container into the cleaning liquid: (a) as a function of the inclined angle at 40℃, (b) as a function of the liquid temperature at 24° inclination.

Ⅳ. Conclusion

Theoretical and numerical analyses of elastic waves have been executed for a high-frequency ultrasonic cleaner which consists of outer and inner containers. The transmission efficiency has been calculated analytically by considering the interactions of waves in the elastic plate of infinite length and liquids in contacts with the plate. Numerical calculations have been performed by combining the finite element analysis of the vibration of the inner container and the boundary element analysis of the acoustic pressure field in the cleaning liquid. In order to maximize the cleaning performance, the conditions to increase the wave transmission through the inner container have been found in terms of several parameters, such as the thickness and inclined angle of the bottom plate of the inner container at a constant temperature of the cleaning liquid and the temperature of the cleaning liquid at the given thickness and inclined angle of the bottom plate.

References

1. K. Morita, *Ultrasonic Cleaning*, Kindai Henshu Ltd, Tokyo, 1989 (in Japanese).
2. J. O. Kim, J. H. Kim, J. Y. Choi, and M. J. Jho, "A study on improving the life and performance of an ultrasonic cleaner by vibration and acoustic analyses," *Transactions of the Korean Society of Mechanical Engineers*, Vol. 19, No. 11, pp. 2939-2953, 1995 (in Korean).
3. Q. Qi and G. J. Brereton, "Mechanisms of removal of micron-sized particles by high-frequency ultrasonic waves," *IEEE Transactions on Ultrasonics, Ferroelectrics, and Frequency Control*, Vol. 42, No. 4, pp. 619-629, 1995.
4. A. Mayer and S. Shwartzman, "Megasonic cleaning: A new cleaning and drying system for use in semiconductor processing," *Journal of Electronic Materials*, Vol. 8, No. 6, pp. 855-864, 1979.
5. H. Hatano and S. Kanai, "High-frequency ultrasonic cleaning tank utilizing oblique incidence," *IEEE Transactions on Ultrasonics, Ferroelectrics, and Frequency Control*, Vol. 43, No. 4, pp. 531-535, 1996.
6. J. D. Achenbach, Wave Propagation in Elastic Solids, North-Holland Publishing, Amsterdam, pp. 220-226, 1975.
7. I. A. Viktorov, *Rayleigh and Lamb Waves*, Plenum Press, New York, pp. 67-83, pp. 117-121, 1967.
8. R. C. Weast, M. J. Astle, and W. H. Beyer, *CRC Handbook of Chemistry and Physics*, 68th ed., CRC Press, Florida, p. F58 , 1988.
9. F. H. Sanders, "Transmission of Sound Through Thin Plates," *Canadian Journal of Research*, Vol. 17, Sec. A, No. 9, pp. 179-193, 1939.

Appendix

The elements H_{ij} of the 6×6 matrix $[H]$ in Eq. (12) are as follows.

$$H_{11} = -H_{21} = q\ \mathrm{sihn}(qd) \qquad H_{12} = H_{22} = q\cosh(qd)$$
$$H_{13} = H_{23} = ik\cosh(sd) \qquad H_{14} = -H_{24} = ik\sinh(sd)$$
$$H_{15} = -ik\cos\theta_1 \exp(ik_1\cos\theta_1) \qquad H_{16} = H_{56} = 0$$
$$H_{25} = H_{65} = 0 \qquad H_{26} = ik_2\cos\theta_2 \exp(ik_2\cos\theta_2)$$
$$H_{31} = -H_{41} = -(k^2+s^2)\cosh(sd) \qquad H_{32} = H_{42} = 2ikq\cosh(qd)$$
$$H_{33} = H_{43} = -(k^2+s^2)\cosh(sd) \qquad H_{34} = -H_{44} = -(k^2+s^2)\sinh(qd)$$
$$H_{35} = H_{36} = 0 \qquad H_{45} = H_{46} = 0$$
$$H_{51} = -H_{61} = (k^2+s^2)\cosh(qd) \qquad H_{52} = -H_{62} = (k^2+s^2)\sinh(qd)$$
$$H_{53} = -H_{63} = 2iks\sinh(sd) \qquad H_{54} = H_{64} = 2iks\cosh(sd)$$
$$H_{55} = -(\rho_1/\rho)k_T{}^2 \exp(ik_1\cos\theta_1) \qquad H_{66} = -(\rho_2/\rho)k_T{}^2 \exp(ik_2\cos\theta_2)$$

▲Sunghoon Choi

Sunghoon Choi has completed his M.S. and Ph.D degrees in the theoretical and applied mechanics program of Northwestern University in 1992 and 1995 respectively. Since then he has been working for Samsung Advanced Institute of Technology. His research interests are in the area of vibro-acoustics, specifically, the fluid-structure interaction problems and analysis of complex submerged structures. He received his bachelor's degree in mechanical engineering from KAIST in 1990.

▲Jin Oh Kim

Jin Oh Kim was born in Seoul in 1958. He received the B.S. and M.S. degrees in mechanical engineering from Seoul National University in 1981 and 1983, respectively, and the Ph.D. degree from the University of Pennsylvania, U.S.A. in 1989.

From 1983 to 1985, he was with the Korea Research Institute of Standards and Science. He was working in the Center for Quality Engineering and Failure Prevention at Northwestern University as a post-doctoral research associate and later as a research assistant professor from 1989 to 1994. He has been working at Samsung Advanced Institute of Technology as a principal researcher since 1994.

His research interests are the applications of ultrasound, such as ultrasonic cleaning and ultrasonic nondestructive evaluation, and the application of the vibroacoustic phenomena, such as loudspeakers, etc.

▲Yong-Hoon Kim

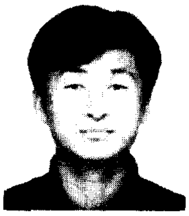

Yong Hoon Kim recived his bachelor's degree in metal engineering from Hanyang University in 1988. He has been working for Samsung Semiconductor R/D Center since 1991 and is currently in charge of back-end of the photomask technology. He is mainly interested in micro cleaning technology.